

Unified Framework for Dislocation-Based Defect Energetics

J. M. Rickman

*Department of Materials Science and Engineering,
Lehigh University, Bethlehem, PA 18015, USA*

Jorge Viñals

*McGill Institute for Advanced Materials and Department of Physics,
3600 University St, Montreal, QC H3A 2T8, Canada*

R. LeSar

Theoretical Division, Los Alamos National Laboratory, Los Alamos, NM 87545, USA

(Dated: February 2, 2008)

Abstract

We present a unified framework for the calculation of defect energies for those defects that can be represented as a superposition of isolated dislocations, and obtain both self and interaction energies of combinations of grain boundaries and cracks. We recover in special limits several well known quantities such as the energy of a low-angle tilt boundary, as well as other lesser known results, including boundary/boundary and crack/boundary interaction energies. This approach, in combination with simple dimensional analysis, permits the rapid calculation of defect energetics in the elastic limit.

PACS numbers: 61.72.Bb

Keywords: Dislocation Density Tensor; Multipole Moments

I. INTRODUCTION

The presence of extended defects in crystalline solids, such as grain boundaries and cracks, can dramatically affect their mechanical response. For example, in large-grained polycrystalline materials, grain boundaries may sometimes impede dislocation motion with a concomitant increase in yield strength,^{1,2} while sharp cracks are stress concentrators that may initiate material fracture^{3,4}. From a micromechanical point of view, the elastic fields associated with grain boundaries or cracks lead to defect interactions that influence fracture behavior in highly-flawed systems and solute segregation^{5,6}, thereby affecting strengthening or embrittling mechanisms.

Calculations of extended defect interaction energies most often begin with the solution of the appropriate elastic boundary value problem, followed by the construction of the corresponding energy density in terms of the stress (or strain) fields and elastic constants and the integration of this density over some volume of space. An alternative approach to the defect interaction problem follows from a micromechanical model of the defect and is based in the elastic Green function of the medium. Such an approach was pioneered by Mura and others^{7,8}, and will be applied here to defects that may be regarded, in some limit, as composed of elemental straight dislocations. As will be seen below, this formalism permits the straightforward calculation of interaction energies for different extended defects and, moreover, facilitates an intuitive, multipole-based analysis that reveals their asymptotic dependence on defect separation.

We address in this paper two prototypical systems: grain boundaries and cracks, as these defects can often be modeled in terms of spatial distributions of line defects, the former typically by regular array(s) of straight dislocations each having a constant Burgers vector, and the latter by a continuous, localized distribution of dislocations with a Burgers vector density depends upon loading conditions. Thus, the eigenstrains corresponding to each defect are conveniently expressed in terms of a dislocation density tensor that embodies the relevant defect length scales and separations. For the purposes of illustration we consider the energetics of a low-angle tilt boundary, the interaction between tilt boundaries, the energetics of an array of cracks, and the interaction between an isolated crack and a grain boundary.

The application of this approach to other, related examples is then discussed.

II. FORMALISM AND SELECTED ILLUSTRATIONS

As indicated above, our calculations are facilitated by describing a defect (e.g., grain boundary, crack) in terms of a dislocation density tensor, $\bar{\rho}^7$. This solenoidal, second-rank tensor carries both local Burgers vector and line direction information, with a divergenceless condition that is a consequence of the topological constraint of line continuity. For example, the components of the density tensors corresponding to straight edge and screw dislocations at $r_1 = r_2 = 0$ with Burgers vectors \vec{b} , and line directions along r_3 are given, respectively, by

$$\begin{aligned}\rho_{ij}(\vec{r}) &= b \delta_{i3} \delta_{jJ} \delta(r_1) \delta(r_2), \quad (\text{edge}, J = 1, 2) \\ \rho_{ij}(\vec{r}) &= b \delta_{i3} \delta_{j3} \delta(r_1) \delta(r_2), \quad (\text{screw}).\end{aligned}\tag{1}$$

Note that, in the first equation, it is assumed that the Burgers vector is aligned either along r_1 or r_2 , and so an arbitrary alignment in the plane may be constructed from appropriate linear combinations. $\delta(r)$ is the Dirac delta function.

The elastic energy of the system $E[\bar{\rho}]$ can be written as a functional of $\bar{\rho}$, as shown by Kosevich and others⁹ and, more recently, has been employed by Nelson and Toner¹⁰ to investigate the effect of unbound dislocation motion on shear response in solids, by Rickman and Viñals¹¹ to model the collective motion of dislocation ensembles, and by Rickman and LeSar¹² to quantify the temperature dependent interaction of fluctuating dislocation lines. For our purposes, it is convenient to express the energy functional for an elastically isotropic medium with shear modulus μ and Poisson ratio ν as the Fourier integral

$$E[\bar{\rho}] = \frac{\mu}{2(2\pi)^3} \int d^3q \frac{1}{q^2} K_{ijkl}(\vec{q}) \tilde{\rho}_{ij}(\vec{q}) \tilde{\rho}_{kl}(-\vec{q}),\tag{2}$$

where the integration is over reciprocal space (tilde denoting a Fourier transform), the kernel (without defect core energy contributions) is given by

$$K_{ijkl} = \left[Q_{ik} Q_{jl} + C_{il} C_{kj} + \frac{2\nu}{1-\nu} C_{ij} C_{kl} \right],\tag{3}$$

and \bar{Q} and \bar{C} are longitudinal and transverse projection operators, defined by

$$\begin{aligned} Q_{ij} &= \delta_{ij} - \frac{q_i q_j}{q^2} \\ C_{ij} &= \epsilon_{ijl} \frac{q_l}{q}, \end{aligned} \quad (4)$$

respectively¹⁰, where δ_{ij} is the Kronecker delta, and ϵ_{ijk} is the Levi-Civita tensor. We note that it is possible to include defect core energies in a somewhat *ad hoc* fashion by augmenting this kernel by a term quadratic in the dislocation density¹⁰. A somewhat more realistic description of the core could be given by an energy term that depends on atomic coordinates, although we will not consider such core models as they fall outside of the mesoscopic description outlined here. As illustrated below, the distance dependence of the defect energy can be determined in a straightforward manner from Eq. (2) by employing a superposition of prototypical densities.

A. Edge Dislocation Arrays - Low-Angle Tilt Grain Boundaries

Consider first a linear array of N edge dislocations, each separated from its nearest neighbor by ℓ and having a Burgers vector aligned along either the r_1 or r_2 axes ($J = 1$ or 2 , respectively), as shown in Fig. 1a. As is well known, this system, with $J = 1$ and in the limit $N \rightarrow \infty$, is a model of a low-angle tilt grain boundary where, in the limit of small grain misorientation angle Θ , $\ell \approx b/\Theta$ ¹³. From Eq. (2) the dislocation density is

$$\rho_{ij}(\vec{r}) = b \delta_{i3} \delta_{jJ} \delta(r_1) \sum_n \delta(r_2 - n\ell), \quad (5)$$

where the summation is over all dislocations in the array. For convenience, we will work with the corresponding Fourier transform

$$\tilde{\rho}_{ij}(\vec{q}) = 2\pi b \delta(q_3) \sum_n \exp(iq_2 n\ell) \delta_{i3} \delta_{jJ}. \quad (6)$$

Before calculating the corresponding boundary energy, we note that singularities inherent in this continuum model that lacks a short distance cut-off lead to a divergent self-energy. The origin of the divergence is the fact that the energy density of a single edge dislocation diverges like $1/r$, where r is the radial distance to the dislocation line. In reality, each

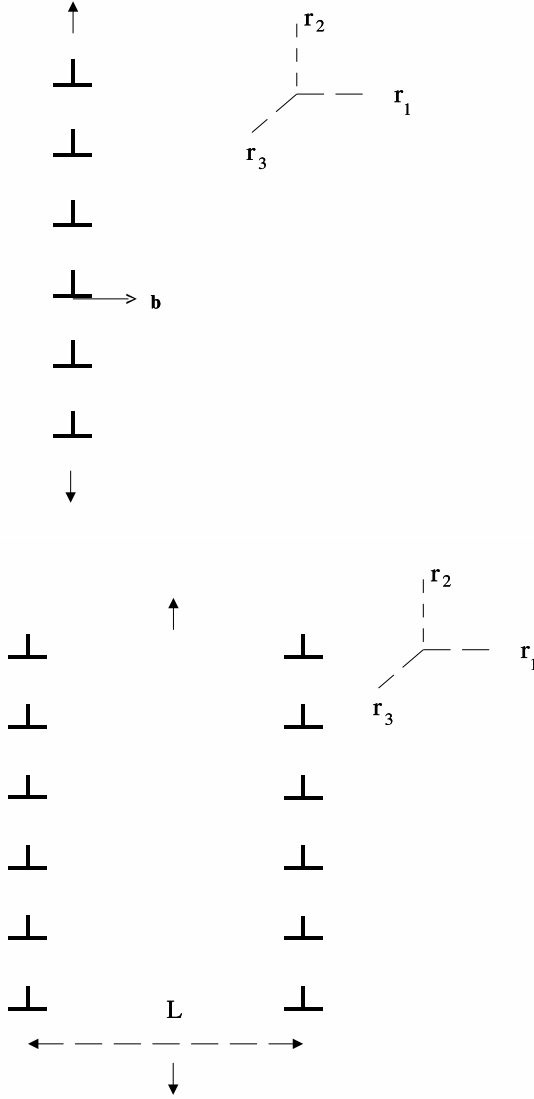


FIG. 1: a.) A low-angle, tilt grain boundary modeled as an array of edge dislocations. Each dislocation has a Burgers vector \vec{b} and is separated from its nearest neighbor by $\ell \approx b/\Theta$ for small misorientation angle Θ . b.) Two such grain boundaries separated by a distance L .

dislocation has an atomic core region that is not amenable to a continuum description. We introduce a small cutoff parameter a representing the core radius by replacing the real-space delta function by the broadened delta representation¹⁴

$$\Delta(r_2 - n\ell) = \frac{a}{\pi} \frac{1}{a^2 + (r_2 - n\ell)^2}. \quad (7)$$

The corresponding Fourier transform can be obtained by using the shifting property of transforms to obtain

$$\tilde{\Delta}(q_2) = \exp(iq_2 n \ell) \exp(-a|q_2|). \quad (8)$$

Therefore the elastic energy of the array of edge dislocations is

$$E_J = \frac{\mu}{2(2\pi)^3} \int d^3 q \frac{1}{q^2} K_{3J3J}(\vec{q}) \tilde{\rho}_{3J}(\vec{q}) \tilde{\rho}_{3J}(-\vec{q}), \quad (9)$$

where

$$K_{3J3J}(\vec{q}) = Q_{33}Q_{JJ} + \frac{1+\nu}{1-\nu} C_{3J}C_{3J} \quad (10)$$

and $J = 1$ or 2 (no summation) denotes the orientation of the Burgers vectors. More specifically, noting that $q^2 = q_1^2 + q_2^2$,

$$K_{3J3J}(\vec{q}) = \left(\frac{2}{1-\nu} \right) \frac{q^2 - q_J^2}{q_1^2 + q_2^2}, \quad (11)$$

and the energy per unit length in the r_3 direction is given by

$$e_J = \frac{\mu b^2}{(2\pi)^2 (1-\nu)} \int \int d^2 q \frac{q^2 - q_J^2}{(q_1^2 + q_2^2)^2} S(q_2) \exp(-2a|q_2|), \quad (12)$$

where a structure factor $S(q_2)$ has been defined as $S(q_2) = |\sum_n \exp(iq_2 n \ell)|^2 = N(2\pi/\ell) \sum_m \delta(q_2 - 2\pi m/\ell)^{15}$. Explicitly we have

$$\begin{aligned} e_1 &= \frac{N\mu b^2}{(2\pi)(1-\nu)\ell} \sum_{m=-\infty}^{\infty} \exp(-4\pi a|m|/\ell) \int dq_1 \frac{(2\pi m/\ell)^2}{(q_1^2 + (2\pi m/\ell)^2)^2}, \\ e_2 &= \frac{N\mu b^2}{(2\pi)(1-\nu)\ell} \sum_{m=-\infty}^{\infty} \exp(-4\pi a|m|/\ell) \int dq_1 \frac{q_1^2}{(q_1^2 + (2\pi m/\ell)^2)^2}. \end{aligned} \quad (13)$$

Upon evaluating the first integral in Eq. (13), one finds

$$e_1 = \frac{N\mu b^2}{2(2\pi)(1-\nu)} \sum_{m=1}^{\infty} \frac{\exp(-4\pi a|m|/\ell)}{|m|}, \quad (14)$$

and therefore

$$e_1 = -\frac{N\mu b^2}{(4\pi)(1-\nu)} \ln[1 - \exp(-4\pi a/\ell)] \approx \frac{N\mu b^2}{(4\pi)(1-\nu)} \ln \left[\frac{\ell}{4\pi a} \right], \quad (15)$$

where the latter approximation holds when a/ℓ is small. If this array represents a planar defect (i.e., grain boundary) then the corresponding energy per unit boundary area is

$$\gamma = \frac{e_1}{N\ell} \approx \frac{\mu b^2}{(4\pi\ell)(1-\nu)} \ln \left[\frac{\ell}{4\pi a} \right]. \quad (16)$$

This result has the same functional form as the classic Read-Shockley energy for a low-angle tilt boundary, though the constant in the argument of the logarithm depends on the details of the short-range (core) cutoff employed here¹³. In this regard, we note that a similar approach to this problem for two-dimensional systems has been outlined elsewhere¹⁶.

Finally we examine e_2 for the extended defect for which $\vec{b} \parallel \hat{r}_2$. From Eq. (13) it is clear that $e_2 \rightarrow \infty$ owing to the divergence associated with the $m = 0$ mode. This result is expected since some components of the long-ranged stress field (namely σ_{22}) tend to a constant as $x \rightarrow \infty$, and thus the volume integral over the energy density diverges in an infinite system. Given this behavior, it is evident that a low-angle boundary with this geometry cannot have dislocations with Burgers vector components in the boundary plane.

B. Dislocation Array Interactions

Consider next two low-angle, symmetric, tilt boundaries separated by a distance L , as shown in Fig. 1b. The interaction energy for these boundaries follows from the corresponding dislocation density tensor

$$\rho_{ij}(\vec{r}) = b\delta_{i3}\delta_{j1} \left[\delta(r_1) \sum_n \delta(r_2 - n\ell) + \delta(r_1 - L) \sum_m \delta(r_2 - m\ell) \right] \quad (17)$$

that can be transformed to yield

$$\tilde{\rho}_{ij}(\vec{q}) = (2\pi b)\delta_{i3}\delta_{j1}\delta(q_3) \left[\sum_n \exp(iq_2 n\ell) + \exp(iq_1 L) \sum_m \exp(iq_2 m\ell) \right] \quad (18)$$

The interaction energy for separated dislocation distributions is obtained from the cross terms (i.e., no self-energies) in Eq. (2). Following the procedure outlined above, one first calculates the interaction energy per unit length of dislocation line

$$e_{int} = \frac{N\mu b^2}{\pi(1-\nu)\ell} \sum_{m=-\infty}^{\infty} \int dq_1 \frac{(2\pi m/\ell)^2}{(q_1^2 + (2\pi m/\ell)^2)^2} \cos(q_1 L) \exp(-4\pi a|m|/\ell) \quad (19)$$

Upon evaluating this integral one finds that

$$e_{int} = \frac{N\mu b^2}{2(1-\nu)} \sum_{m=1}^{\infty} \left[\left(\frac{L}{\ell} \right) + \left(\frac{1}{2\pi|m|} \right) \right] \exp(-\alpha|m|), \quad (20)$$

where $\alpha = (4\pi a/\ell) + (2\pi L/\ell)$. The resulting summations can also be performed to yield the grain-boundary interaction energy per unit area

$$\gamma_{int} = \frac{e_{int}}{N\ell} = \frac{\mu b^2}{2\pi(1-\nu)\ell} \left[\left(\frac{2\pi L}{\ell} \right) \left(\frac{1}{\exp(\alpha) - 1} \right) - \ln[1 - \exp(-\alpha)] \right] \quad (21)$$

It is of interest to examine γ_{int} for two limiting cases. First, for large boundary separations such that $L/\ell \gg 1$ and $a/\ell \ll 1$, $e_{int} \propto (L/\ell) \exp(-2\pi L/\ell)$. This exponential decay in the interaction energy follows from the rapid (exponential) decay of the stress fields associated with the individual arrays. By contrast, for $L/\ell \sim 1$, the logarithmic dependence of e_{int} on L/ℓ results from individual dislocations in either array “seeing” each other. Finally, we note that an alternative route to Eq. (21) follows from a calculation of the Peach-Koehler force acting on a dislocation owing to a distant array and a subsequent spatial integration to obtain the energy.¹⁷

C. Crack Array

Another application of the formalism presented above is the interaction energy between cracks. We first consider a single crack of length $2c$ oriented along the r_1 axis, and model it as a continuous dislocation distribution, with corresponding dislocation function $B(r_1)$.¹⁸ The Burgers vectors of the dislocations that comprise the crack model embody the local crack opening that results from a given loading. Hence, by choosing an appropriate dislocation distribution, one can represent loading in various modes. Having represented the crack with a dislocation distribution, the stress field associated with the crack is given in terms of the stress field of a single edge dislocation σ_{ij}^\perp by the convolution integral

$$\sigma_{ij}(r_1, r_2) = \int_{-\infty}^{+\infty} dr'_1 B(r'_1) \sigma_{ij}^\perp(r_1 - r'_1, r_2) \quad (22)$$

As a specific example, consider a Mode II crack. The shear loading associated with this mode can be represented by a distribution of edge dislocations with Burgers vectors oriented along r_1 . Thus, one can write $B(r_1) = \int dr_2 \rho_{31}(r_1, r_2)$ for an appropriate dislocation density ρ_{31} that can be determined from the requirement that the crack faces must be traction-free.¹⁸

It is of interest here to consider a crack interacting with distant objects. In particular, given an observation point \vec{r} such that $|\vec{r}|/2c \gg 1$, it is permissible to regard the crack fields

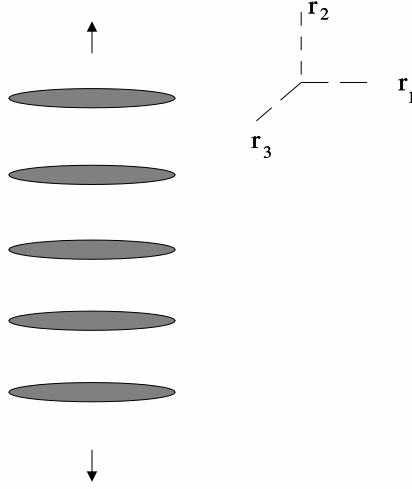


FIG. 2: An array of cracks, each separated from its nearest neighbor by a distance ℓ along the r_2 axis. It is assumed that the system is subjected to a constant shear stress τ . Also shown is a schematic of the dislocation distribution corresponding to each crack.

as produced by the lowest-order multipole moments of $B(r_1)$. In practice, the “monopole” and “dipole” moments are often satisfactory in this context and one obtains

$$\int_{-\infty}^{+\infty} dr_1 B(r_1) = b_{tot}, \quad (23)$$

and,

$$D = \int_{-\infty}^{+\infty} dr_1 r_1 B(r_1) = \frac{-2(1-\nu)}{\mu} \int_{-c}^{+c} dr_1 \sqrt{c^2 - r_1^2} \sigma_{12}(r_1, r_2 = 0), \quad (24)$$

where b_{tot} is the total Burgers vector associated with the crack dislocations and $\sigma_{12}(r_1, r_2 = 0)$ is the shear stress loading the crack.^{18,19}

We now derive the interaction energy associated with various crack arrays. Consider, for example, a linear array of Mode II cracks, each crack closed at both ends (i.e., $b_{tot} = 0$) and modeled as a dislocation dipole in the r_2 direction that is separated from its nearest neighbor by ℓ . As is evident from Eq. (24), and by contrast with the grain-boundary models discussed above, the strength of elemental defects (i.e., their dipole moment) is not fixed, as it depends on the local stress field. The geometry for this loading, as well as the corresponding dislocation orientations, is shown in Fig. 2. In the short crack limit, such that each crack

may be regarded as a point dipole with moment D_ℓ (i.e., the limit $c \rightarrow 0$ and $b \rightarrow \infty$ with $2cb \rightarrow D_\ell$), the corresponding dislocation density tensor is

$$\rho_{31}(\vec{r}) = D_\ell \delta_{i3} \delta_{j1} \delta'(r_1) \sum_n \delta(r_2 - n\ell), \quad (25)$$

where the prime denotes differentiation with respect to the argument, and the subscript ℓ indicates that the dipole moment depends on crack separation. As before, it is convenient to work in reciprocal space where one finds that

$$\tilde{\rho}_{31}(\vec{q}) = 2\pi i D_\ell q_1 \delta(q_3) \sum_n \exp(iq_2 n\ell) \delta_{i3} \delta_{j1} \quad (26)$$

By analogy with the development given above, the energy of this system is given by

$$e_c = \frac{N\mu D_\ell^2}{(2\pi)(1-\nu)\ell} \sum_{m=-\infty}^{\infty} \int dq_1 q_1^2 \frac{(2\pi m/\ell)^2}{(q_1^2 + (2\pi m/\ell)^2)^2} \exp(-4\pi a|m|/\ell). \quad (27)$$

Upon performing the required integral and summation, one finds that

$$e_c = \frac{2\pi N\mu D_\ell^2}{(1-\nu)\ell^2} \frac{\exp(4\pi a/\ell)}{[\exp(4\pi a/\ell) - 1]^2}. \quad (28)$$

It is of interest to examine e_c in the limit of large crack separations ℓ where the dipole approximation works best. One finds that $e_c \rightarrow [N\mu D_\ell^2/8\pi(1-\nu)] [1/a^2 - 4\pi^2/3\ell^2 + O(1/\ell^4)]$, the first term arising from the self-energy of a dislocation dipole, and the second arising from dipole-dipole interactions.

An approximation to D_ℓ for a particular array spacing ℓ may be obtained by requiring that the shear stress traction produced by neighboring cracks on the face of a given crack be compensated by a uniform stress that is the same for every crack in the array. The strategy for such calculations is given elsewhere¹⁹, and the details for this defect geometry are given in Appendix A.

D. Crack-Grain Boundary Interaction

As a final illustration of extended defect energy calculations, consider the interaction of a low-angle grain boundary separated from an isolated crack by a distance L , as shown

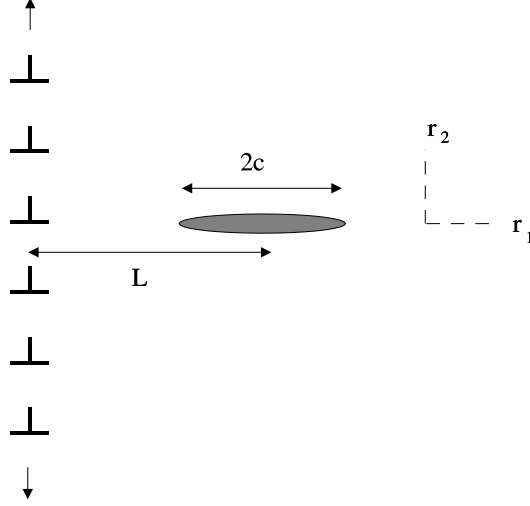


FIG. 3: An isolated crack interacting with a low-angle tilt boundary, the latter modeled as an array of edge dislocations. For simplicity, the crack is located at a distance L from the boundary and at $r_2 = 0$. For this geometry the crack is subjected to shear stresses owing to the grain boundary.

schematically in Fig. 3. For this geometry the normal stress on the crack faces owing to the boundary is $\sigma_{22}(r_1, r_2 = 0) = 0$, while the shear stresses $\sigma_{12}(r_1, r_2 = 0) \neq 0$, and so the crack is loaded in Mode II. From the grain-boundary (Eq. (6)) and crack (Eq. (26)) dislocation densities one can then construct the interaction energy per unit dislocation length, namely

$$e_{cgb} = \sum_n \frac{\mu b D_L}{(2\pi)^2 (1 - \nu)} \int \int d^2 q \frac{q_2^2}{(q_1^2 + q_2^2)^2} i q_1 \exp(i q_1 L) \cos(q_2 n \ell) \exp(-a |q_2|) \quad (29)$$

Evaluating the integrals and the summation, we find that

$$e_{cgb} = \frac{\mu b D_L}{(2\pi)^2 (1 - \nu)} \frac{L \pi^3}{\ell^2} \operatorname{csch}^2 \left[\pi \left(\frac{a + L}{L} \right) \right]. \quad (30)$$

In the limit of $\ell/L \ll 1$, $e_{cgb} \simeq (L/\ell^2) \exp[-2\pi(a + L)/L]$, owing to the exponential decay of the stress fields associated with the grain boundary while, for $\ell/L \simeq 1$ (and $a/L \ll 1$) $e_{int} \simeq 1/L$, consistent with a monopole-dipole interaction. We note that this result can be obtained somewhat more readily by returning to the calculation of the grain boundary interaction energy and considering a single dislocation within a grain boundary array. Since a crack is modeled here as a dislocation dipole one replaces, in effect, an edge dislocation

density with its spatial derivative and therefore the functional form of the crack/boundary interaction energy is given by $L (\partial e_{int}/\partial L)$ (see Eq. (21)).

The crack dipole moment D_L can again be determined from the shear loading conditions via Eq. (24). For the crack geometry shown in Fig. 3, this leads to

$$D_L = \frac{-2b\pi}{\ell^2} \int_{-c}^{+c} dr_1 \sqrt{c^2 - r_1^2} (r_1 + L) \left[\cosh \left(\frac{2\pi (r_1 + L)}{\ell} \right) - 1 \right]^{-1}, \quad (31)$$

where the shear stress is that for an array of edge dislocation.¹³ This integral can be evaluated numerically by a Gauss-Chebyshev integration technique based on type II Chebyshev polynomials.²²

III. CONCLUSIONS

A unified framework for the calculation of defect energies has been presented here and, for the purposes of illustration, applied to several different systems containing grain boundaries and/or cracks. In each case, a set of elemental dislocations comprise the extended defect under consideration, and the corresponding dislocation density is either independent of other defect positions (e.g., grain boundary) or calculable from the stresses imposed by these other defects (e.g., crack). As indicated above, this approach is especially useful in providing an intuitive understanding of interactions based on idealized defect models.

The foregoing development can, of course, be applied to other systems for which a dislocation-based model is appropriate. For example, one can also obtain the energetics of a roughened tilt boundary^{20,21} by considering perturbations of the dislocation density resulting from sinusoidal variations in the position of constituent dislocation lines. If these variations in boundary morphology are temperature induced, this analysis can be used to compute the statistical weights of perturbed boundary configurations to the free energy of the system and, consequently, to deduce a thermodynamic roughening temperature. In addition, the description of more complex, asymmetrical boundary structures, consisting of two or three sets of edge dislocations, or twist boundaries consisting of perpendicular sets of screw dislocations is also possible by a generalization of the structure factor (see below Eq. (12)) to include a form factor that reflects the positions of the basis dislocations within a

unit cell that generates the boundary. These and other calculations will be the subject of a future publication.

Finally, we mention that, for the sake of completeness, Appendix B contains expressions for the stress tensor in the same Fourier representation used here for the energy, along with some simple examples. In a future publication, we will apply a similar formalism as used for the energy to derive equations for the stress arising from extended defects.

Acknowledgments

The authors would like to acknowledge many helpful discussion with Professor T. Delph and Mr. C. Lowe. This research has been supported in part (JV) by the U.S. Department of Energy under contract No. DE-FG05-95ER14566. The work of R. LeSar was performed under the auspices of the United States Department of Energy (US DOE under contract W-7405-ENG-36) and was supported by the Division of Materials Science of the Office of Basic Energy Sciences of the Office of Science of the US DOE.

-
- ¹ A. H. Cottrell, *An Introduction to Metallurgy* (Edward Arnold, London, 1967).
 - ² V. Bata and E. V. Pereloma, “An Alternative Physical Explanation of the Hall-Petch Relation”, *Acta Mater.* **52**, 657-665 (2004).
 - ³ K. Bowman, *Mechanical Behavior of Materials* (John Wiley and Sons, Hoboken, NJ, 2004).
 - ⁴ N. Sridhar, J. M. Rickman, and D. J. Srolovitz, “Thermoelastic Analysis of Matrix Crack Growth in Particulate Composites”, *Acta Metall. Mater.* **43**, 1669 (1995).
 - ⁵ C.-W. Li and W. D. Kingery, “Solute Segregation at Grain Boundaries in Polycrystalline Al_2O_3 ”, in *Advances in Ceramics*, Vol 10., pp. 368-378.
 - ⁶ Q. L. Wang, G. Lian, E. C. Dickey, “Grain Boundary Segregation in Yttrium-Doped Polycrystalline TiO_2 ”, *Acta Mater.* **52**, 809 (2004).
 - ⁷ T. Mura, *Micromechanics of Defects in Solids* (Martinus Nijhoff, Boston, 1987), p. 340.
 - ⁸ C. Teodosiu, *Elastic Models of Crystal Defects* (Springer-Verlag, New York, 1982).

- ⁹ A. M. Kosevich, “Crystal Dislocations and the Theory of Plasticity,” in *Dislocations in Solids*, ed. by F. R. N. Nabarro (North-Holland, New York, 1979), p. 37.
- ¹⁰ D. R. Nelson and J. Toner, “Bond-Orientational Order, Dislocation Loops and Melting of Solids and Smectic-A Liquid Crystals,” *Phys. Rev. B* **24**, 363-387 (1981).
- ¹¹ J. M. Rickman and Jorge Viñals, “Modeling of Dislocation Structures in Materials,” *Phil. Mag. A* **75**, 1251 (1997).
- ¹² J. M. Rickman and R. LeSar, “Dislocation Interactions at Finite Temperature”, *Phys. Rev. B* **64**, 094106 (2001).
- ¹³ J. P. Hirth and J. Lothe, *Theory of Dislocations* (Krieger, Malabar, Florida, 1982).
- ¹⁴ O. L. Alerhand, D. Vanderbilt, R. D. Meade, and J. D. Joannopoulos, “Spontaneous Formation of Stress Domains on Crystal Surfaces”, *Phys. Rev. Lett.* **61**, 1973-1976 (1988).
- ¹⁵ H. Kleinert, *Gauge Fields in Condensed Matter, Vol. II* (World Scientific, Teaneck, NJ, 1989), pp. 1162-1217.
- ¹⁶ P. M. Chaikin and T. Lubensky, *Principles of Condensed Matter Physics* (Cambridge University Press, Cambridge, 1995), p. 256.
- ¹⁷ R. Thomson, M Koslowski, and R. LeSar, “A Comparative Study of Energetics and Noise in Dislocation Patterning,” unpublished.
- ¹⁸ J. Weertman, *Dislocation Based Fracture Mechanics* (World Scientific, River Edge, NJ, 1996).
- ¹⁹ A. V. Dyskin and H.-B. Mühlhaus, “Equilibrium Bifurcations in Dipole Asymptotics Model of Periodic Crack Arrays”, in *Continuum Models for Materials with Microstructure*, ed. by H.-B. Mühlhaus (John Wiley and Sons, New York, NY, 1995), pp 69-104.
- ²⁰ C. Rottman, “Roughening of Low-Angle Grain Boundaries”, *Phys. Rev. Lett.* **57** 735-738 (1986).
- ²¹ C. Rottman, “Thermal Fluctuations in Low-Angle Grain Boundaries”, *Acta Metall.* **34**, 2465-2479 (1986).
- ²² P. J. Davis and P. Rabinowitz, *Methods of Numerical Integration* (Academic Press, NY, 1984).
- ²³ N. I. Muskhelishvili, *Some Basic Problems of the Mathematical Theory of Elasticity* (P. Noordhoff, Groningen, Netherlands, 1953).
- ²⁴ G. B. Arfken and H.-J. Weber, *Mathematical Methods for Physicists* (Academic Press, New York, 2001).

²⁵ The Green function of the biharmonic operator can be obtained by noting that, in infinite space, $\nabla^4|\vec{r}| = \nabla^2\nabla^2|\vec{r}| = -\delta(\vec{r})$. This result follows from the Green function relation for the three-dimensional Laplace operator $\nabla^2|\vec{r}| = -\frac{1}{|\vec{r}|}$.

APPENDIX A: CRACK ARRAYS

An approximation to the stress on a crack needed to balance those owing to others in the linear array shown in Fig. 2 can be obtained via the formalism of Dyskin and Mühlhaus.¹⁹ We follow their approach below, except that the required stress fields are obtained by a multipole expansion rather than by using the Muskhelishvili complex potentials.²³ First, assuming that the crack separation ℓ is large, one can regard each crack as a dislocation dipole. For this geometry the relevant stresses associated with each crack, in the limit of small crack width $2c$, are given in terms of the derivatives of the derivative of the stresses (i.e., a point dipole approximation) for individual dislocations by

$$\sigma_{12}(r_1, r_2) \approx \frac{\mu bc}{\pi(1-\nu)} \frac{\partial}{\partial r_1} \left[\frac{r_1(r_1^2 - r_2^2)}{(r_1^2 + r_2^2)^2} \right] = \frac{\mu D}{2\pi(1-\nu)} \left[\frac{3r_1^2 - r_2^2}{(r_1^2 + r_2^2)^2} - \frac{4r_1^2(r_1^2 - r_2^2)}{(r_1^2 + r_2^2)^3} \right], \quad (\text{A1})$$

and

$$\sigma_{22}(r_1, r_2) \approx \frac{\mu bc}{\pi(1-\nu)} \frac{\partial}{\partial r_1} \left[\frac{r_2(r_1^2 - r_2^2)}{(r_1^2 + r_2^2)^2} \right] = \frac{\mu D r_1 r_2}{\pi(1-\nu)} \left[\frac{1}{(r_1^2 + r_2^2)^2} - \frac{2(r_1^2 - r_2^2)}{(r_1^2 + r_2^2)^3} \right], \quad (\text{A2})$$

where D is the dipole moment. Given the symmetry of the crack array, it is clear that the stresses σ_{22} will cancel upon summation over all cracks.

Next, we invoke a dipole asymptotics approximation¹⁹ in which the i -th crack is subjected to a loading shear stress τ and an additional uniform load ϵ_i , the latter equal to the stresses generated by the other cracks at the center of the i -th crack. The corresponding dipole moment is $D_i = -\pi c^2(1-\nu)(\tau + \epsilon_i)/\mu$. The corrective stress associated with the j -th crack is then given by

$$\epsilon_j = \frac{c^2}{2\ell^2} \sum_{i \neq j} \frac{1}{(i-j)^2} (\tau + \epsilon_i). \quad (\text{A3})$$

Finally, taking each crack to be identical so that $\epsilon_i = \epsilon$ and using the Riemann zeta function

relation $\sum_{n=1}^{\infty} 1/n^2 = \zeta(2) = \pi^2/6$,²⁴ one finally obtains

$$\epsilon = \tau \frac{(c/\ell)^2 \zeta(2)}{1 - (c/\ell)^2 \zeta(2)}. \quad (\text{A4})$$

The dipole moment can now be expressed in terms of τ and ϵ .

APPENDIX B: STRESS TENSOR

The stress tensor can also be given in terms of the dislocation density tensor. As discussed by Kosevich⁹, the stress field at point \vec{r}

$$\sigma_{ik}(\vec{r}) = 2\mu \left[\nabla^2 \chi'_{ik} + \frac{1}{1-\nu} \left(\frac{\partial^2 \chi'_{il}}{\partial x_i \partial x_k} - \delta_{ik} \nabla^2 \chi'_{il} \right) \right], \quad (\text{B1})$$

with

$$\chi'_{ik} = -\frac{1}{8\pi} \int |\vec{r} - \vec{r}'| \eta_{ik}(\vec{r}') d\vec{r}', \quad (\text{B2})$$

and

$$\eta_{ik} = \frac{1}{2} \left[\epsilon_{ipl} \frac{\partial \rho_{kl}}{\partial x_p} + \epsilon_{kpl} \frac{\partial \rho_{il}}{\partial x_p} \right]. \quad (\text{B3})$$

In Fourier space one can write Eq. (B2) as

$$\tilde{\chi}'_{ik}(\vec{q}) = \tilde{G}(\vec{q}) \tilde{\eta}_{ik}(\vec{q}), \quad (\text{B4})$$

with $\tilde{G}(\vec{q}) = 1/q^4$, the Green function of the biharmonic operator²⁵. Furthermore,

$$\tilde{\eta}_{ik}(\vec{q}) = \frac{i}{2} [\epsilon_{ipl} q_p \rho_{il}(\vec{q}) + \epsilon_{kpl} q_p \rho_{il}(\vec{q})] = -\frac{iq}{2} [C_{il} \rho_{kl}(\vec{q}) + C_{kl} \rho_{il}(\vec{q})]. \quad (\text{B5})$$

Given these transforms, the Fourier transform of the stress tensor can be written, after some algebra, as

$$\tilde{\sigma}_{ik}(\vec{q}) = i\mu q^3 \tilde{G}(\vec{q}) \left(C_{il} \rho_{kl} + C_{kl} \rho_{il} - \frac{2}{1-\nu} Q_{ik} C_{al} \rho_{al} \right). \quad (\text{B6})$$

To illustrate the use of Eq. (B6), consider the case of a single straight screw dislocation, aligned along r_3 and having Burgers vector \vec{b} . The corresponding dislocation density is $\tilde{\rho}_{kl} = 2\pi b \delta_{k3} \delta_{l3} \delta(q_3)$.

Upon substituting this density into Eq. (B6) one finds that

$$\tilde{\sigma}_{ik}(\vec{q}) = 2\pi i\mu q^3 \tilde{G}(\vec{q}) b \delta(q_3) (C_{i3} \delta_{k3} + C_{k3} \delta_{i3}). \quad (\text{B7})$$

Therefore, one immediately sees that $\tilde{\sigma}_{11} = \tilde{\sigma}_{22} = \tilde{\sigma}_{33} = 0$, and that $\tilde{\sigma}_{12} = 0$. The non-vanishing stress component

$$\tilde{\sigma}_{13} = -i2\pi\mu b \left(\frac{q_2}{q^2} \right) \delta(q_3). \quad (\text{B8})$$

and so, in real space,

$$\sigma_{13} = -\frac{\mu b y}{2\pi r^2}. \quad (\text{B9})$$

A similar result can be derived for σ_{23} .